J. Biochem. **143,** 505–515 (2008)
doi:10.1093/jb/mvm241

Functional Characterization of the Recombinant Group II Chaperonin α from *Thermoplasma acidophilum*

Hidenori Hirai[2], Kentaro Noi[2], Kunihiro Hongo[1,2], Tomohiro Mizobata[1,2] and Yasushi Kawata[1,2,*]

[1]Department of Biotechnology, Faculty of Engineering; and [2]Department of Biomedical Science, Institute of Regenerative Medicine and Biofunction, Graduate School of Medical Science, Tottori University, Tottori 680-8552, Japan

Received November 14, 2007; accepted December 18, 2007; published online January 2, 2008

The functional characteristics of group II chaperonins, especially those from archaea, have not been elucidated extensively. Here, we performed a detailed functional characterization of recombinant chaperonin α subunits (16-mer) (Ta-cpn α) from the thermophilic archaea *Thermoplasma acidophilum* as a model protein of archaeal group II chaperonins. Recombinant Ta-cpn α formed an oligomeric ring structure similar to that of native protein, and displayed an ATP hydrolysis activity (optimal temperature: 60°C) in the presence of either magnesium, manganese or cobalt ions. Ta-cpn α was able to bind refolding intermediates of *Thermus* MDH and GFP in the absence of ATP, and to promote the refolding of *Thermus* MDH at 50°C in the presence of Mg^{2+}-, Mn^{2+}-, or Co^{2+}-ATP. Ta-cpn α also prevented thermal aggregation of rhodanese and luciferase at 50°C. Interestingly, Ta-cpn α in the presence of Mn^{2+} ion showed an increased hydrophobicity, which correlated with an increased efficiency in substrate protein binding. Our finding that Ta-cpn α chaperonin system displays folding assistance ability with ATP-dependent substrate release may provide a detailed look at the potential functional capabilities of archaeal chaperonins.

Key words: archaeal chaperonin, chaperonin activity, metal ion, protein folding, *Thermoplasma acidophilum*.

Abbreviations: ANS, 8-anilino-1-naphthalene sulfonic acid; CCT, chaperonin containing t-complex polypeptide; Gdn-HCl, guanidine hydrochloride; GFP, green fluorescent protein; MDH, malate dehydrogenase; Ta-cpn α, recombinant chaperonin that is comprised of 16 α-subunits from *Thermoplasma acidophilum*.

Chaperonin proteins play a pivotal role in assisting the folding of newly synthesized polypeptides and stress-denatured proteins, and are well conserved in every living organism (*1*, *2*). Chaperonins share homologous amino acid sequences and form a double-ring structure, in which the folding of nascent polypeptide and denatured protein is mediated in an ATP-dependent manner (*2*, *3*). Chaperonins are divided into two groups; group I chaperonins represented by GroEL found in bacteria, mitochondria and chloroplasts, and group II chaperonins found in archaea and eukaryotic cytosol (*2*, *4*).

Group I chaperonins such as GroEL from *Escherichia coli* exist in the cell as a homo-tetradecamer (60 kDa subunit × 14), consisting of two 7-fold symmetrical rings. GroEL requires a co-chaperonin, GroES (7-mer) to fulfil the chaperonin function (*1*, *5*); GroEL binds denatured proteins and facilitates their folding by encapsulating them within the central cavity in co-operation with the co-chaperonin GroES (7-mer) in the presence of ATP. Thus, the chaperonin GroEL protects denatured proteins from interactions with other misfolded proteins or aggregation prone species, providing the proper environment in which the denatured protein may fold spontaneously (*2*, *6*, *7*).

In contrast, group II chaperonins from archaea form double-ring cylinders with an 8-fold or 9-fold symmetry, consisting of 1–3 types of subunit (*4*). For example, *Pyrococcus furiosus* (*8*), *Pyrococcus horikoshii* OT3 (*9*), *Methanococcus jannaschii* (*10*), *Methanopyrus kandleri* (*11*) and *M. thermolithotrophicus* (*12*) have only a single chaperonin subunit type; in each case a homo-hexadecamer is formed by two eight-membered rings. On the other hand, *Thermococcus* strain KS-1 (*13*), *Pyrococcus kodakaraensis* KOD1 [*Thermococcus kodakaraensis* KOD1 (*14*)] (*15*), *Pyrodictium occultum* (*16*), *Aeropyrum pernix* K1 (*17*) and *Thermoplasma acidophilum* (*18*, *19*) have two subunit types, α and β; two eight-membered rings of $(\alpha\beta)_4$ form a hetero-hexadecamer. From phylogenetic analyses, it is also reported that *Sulfolobus* species has three different types of chaperonin subunit, and *Sulfolobus shibatae* and *Sulfolobus solfataricus* form nine-membered rings (*20*). Moreover, the eukaryotic group II chaperonin, CCT, consists of eight homologous but unique subunits, which form a hetero-oligomeric double ring complex (*4*).

The functional characteristics of eukaryotic group II chaperonins have been gradually clarified. The eukaryotic CCT is found to be essential for correct folding of an

*To whom correspondence should be addressed. Tel: +81 857 31 5271, Fax: +81 857 31 5271, E-mail: kawata@bio.tottori-u.ac.jp

important subset of cytosolic proteins, including cytoskeletal components such as actin, tubulin and cell cycle regulators (*2*, *21–26*). Recent studies demonstrated that CCT recognized poly-glutamine expanded huntingtin exon-1 soluble oligomers, as well as the yeast G-protein homolog, Gβ hydrophobic β strand, and promoted their non-toxic oligomeric assembly in conjunction with Hsp70 system proteins (*27–29*). The aggregation states of these proteins were altered by the specific interaction of CCT (*27*, *30*). Furthermore, it was reported that the substrate binding region of CCT is localized at a helical region in the apical domain analogous to that found in bacterial chaperonins (*31*).

Studies on the functional characteristics of archaeal group II chaperonins have not advanced as rapidly as CCT, in spite of detailed information on their structural aspects. One of the reasons for this may be related to the fact that most archaeal chaperonins form tight complexes with substrate proteins and subsequently fail to release them *in vitro*. In the case of *T. acidophilum* chaperonin, X-ray structural analysis and molecular characterization have been performed (*32*). The chaperonin forms a double-toroidal $(\alpha\beta)_4(\alpha\beta)_4$ structure, and it exhibited a weak ATP hydrolysis activity and denatured protein binding ability. However, it formed tight complexes and failed to refold the bound substrate protein (*19*). Both native and recombinant αβ *T. acidophilum* chaperonins have been studied with regard to structural characteristics, such as conformational changes caused by ATP-hydrolysis and subunit cooperativity (*33–38*). Due to difficulties in the simultaneous expression of α and β subunits, expression of the genes were performed separately, and it was found that α and β subunits were both able to form homo-oligomeric structures similar to the native chaperonin (*39*). However, the β-subunit oligomer was found to be less stable than the α-subunit oligomer. Although the structural changes and the cooperativity of the α subunit oligomer were studied in the presence of ATP (*36*, *40*), the folding-assistance functions have not been probed. Whether these homo-oligomeric chaperonins possesses abilities to bind substrate proteins and to mediate protein folding remains an open question.

In this study, we report the functional characteristics of recombinant homo-oligomeric *T. acidophilum* α-subunit chaperonin (Ta-cpn α), as a model for archaeal group II chaperonin function. We found that Ta-cpn α showed an ATP hydrolysis activity that was dependent upon various divalent metal ions (Mg^{2+}, Mn^{2+} and Co^{2+}), as well as a refolding assistance activity toward thermophilic malate dehydrogenase (MDH). Ta-cpn α was able to bind refolding intermediates of MDH and GFP in the absence of ATP. Interestingly, the structure of Ta-cpn α in the presence of Mn^{2+} ion showed an increased hydrophobicity, which correlated to an increased efficiency in the ability to bind substrate proteins. It was also found that Ta-cpn α protected rhodanese and luciferase from thermal aggregation. This finding is a first report, to our knowledge, documenting the functional abilities of the chaperonin α-subunit from *T. acidophilum*. Our results are very important in understanding the structural and functional mechanism of archaeal group II chaperonins.

MATERIALS AND METHODS

Cloning, Expression and Purification of Ta-cpn α—The structural gene (*T. acidophilum* Ta0980) of *T. acidophilum* chaperonin α-subunit was amplified from genomic DNA by PCR (*18*) and inserted into pET23a(+) vector (Novagen). The amplified gene was confirmed by DNA sequence analysis. For expression of Ta-cpn α, *E. coli* BL21(DE3) cells were transformed with the constructed plasmid and grown at 37°C in LB medium in the presence of 50 μg/ml ampicillin over night. For purification of Ta-cpn α, harvested cells were resuspended in Buffer A (50 mM Hepes-KOH, pH 7.4, containing 2 mM EDTA, 1 mM DTT and 1 mg/ml Pefabloc) and lysed by sonication on ice and centrifuged. The supernatants were heated at 55°C for 30 min and cooled immediately on ice. Heat aggregated proteins were removed by centrifugation and filtration. Soluble proteins were then loaded onto a Resource-Q anion exchange column (GE Healthcare), which had been equilibrated with Buffer B (50 mM Hepes-KOH, pH 7.4, containing 2 mM EDTA, 1 mM DTT and 1 mM phenylmethylsulfonyl fluoride), and eluted with a 0–600 mM KCl linear gradient using an ÄKTA-FPLC system at 4°C. Fractions containing Ta-cpn α were pooled and concentrated using Amicon-10 (*Mw* 10,000 cut off filter). The preparations were loaded onto Superdex 200 HR 10/30 or Superdex 200 10/300 GL columns (GE Healthcare) equilibrated with Buffer C (50 mM Hepes-KOH, pH 7.4, containing 150 mM KCl). Ta-cpn α was eluted after the void volume, and a monomeric Ta-cpn α subunit fraction was eluted later. The purity of Ta-cpn α protein was confirmed by 15% SDS–PAGE, and the protein was identified by analysis of the N-terminal amino acid sequence on a SHIMADZU PPSQ-10 protein sequencer. Protein concentrations of purified Ta-cpn α were determined by using the commercial Protein Assay Kit (Bio-Rad) with BSA as a standard.

Determination of Ta-cpn α Molecular Mass and Transmission Electron Microscopy (TEM) Measurements—Molecular mass was determined using a Superdex 200 10/300 GL column (GE Healthcare) equilibrated with Buffer C on an ÄKTA-FPLC system at 4°C.

TEM measurements were performed on a JEOL-1210 transmission electron microscope operated at 80 kV. Observation of recombinant Ta-cpn α chaperonin was carried out at a magnification of 150,000 and further magnified (×10) by monitor display. Sample protein concentrations of 0.05 mg/ml were used and negatively stained with 2% (w/v) uranyl acetate solution using copper grids (400-mesh) covered by carbon coated collodion film (Nissin EM).

pH Adjustment—The actual pH of each buffer at the respective temperatures was adjusted for temperature-dependent shifts, by estimating that one degree of temperature increase would result in a shift of −0.014 pH units for Hepes (*41*).

Nucleotide Hydrolysis Activity—Nucleotide hydrolysis activity measurement was performed routinely as follows. Reaction mixtures containing 0.3 μM Ta-cpn α in reaction buffer (50 mM Hepes-KOH, pH 7.0, containing 10 mM KCl and one of the following chloride salts;

5 mM $MgCl_2$, $MnCl_2$, or $CoCl_2$) were incubated for 90 min at 60°C. For experiments to probe ATP hydrolysis activity enhancement by NH_4^+ and optimal temperature analysis, the buffer containing 5 mM $MgCl_2$ and 0.5–2M NH_4Cl were incubated for 10 min at various temperatures. The reaction was started by addition of 2 mM nucleotide. At appropriate intervals, 50 μl reaction mixture was withdrawn and mixed with 550 μl stop solution (7% perchloric acid). After standing on ice for 30 min, the solution was centrifuged by 20,000 × g for 10 min at 4°C, and the supernatant was used for assays. The quantity of inorganic phosphate (Pi) produced during the reaction was determined colorimetrically with the malachite green reagent (*42*).

Refolding of Thermus sp. MDH and GFP—Refolding assistance abilities of Ta-cpn α were probed using the refolding reactions of *Thermus* sp. MDH (*M*w 35,000 × dimer) and GFP (*M*w 29,500 × monomer). *Thermus* sp. MDH was purchased from AMANO ENZYME Inc. (Nagoya, Japan). *Thermus* MDH was unfolded as follows: *Thermus* MDH (5.2 μM MDH monomer) was incubated in 37.5 mM Hepes-KOH, pH 7.0, containing 6M Gdn-HCl at 50°C for 30 min. Refolding was started by 200-fold dilution of this denatured *Thermus* MDH sample into buffer (50 mM Hepes-KOH, pH 7.0, containing 10 mM KCl and either 5 mM $MgCl_2$, 5 mM $MnCl_2$, or 2 mM $CoCl_2$) containing either 0.026 μM or 0.17 μM Ta-cpn α oligomer at 50°C (concentration of MDH during refolding: 0.026 μM monomer). In experiments where the molar ratio of chaperonin oligomer to MDH monomer was equivalent, 2 mM (final concentration) ATP was immediately added after the refolding reaction was started. In experiments where an excess of chaperonin was present relative to MDH, various nucleotides at a concentration of 2 mM was added after 5 min. At the indicated time points, 50 μl of the reaction mixture was taken and added to 1,450 μl assay buffer (50 mM Hepes-KOH, pH 7.0, containing 10 mM KCl, 270 μM β-NADH and 270 μM oxaloacetate) pre-incubated at 25°C. Refolding yields were determined by monitoring the decrease in absorbance of 340 nm at 25°C using a Hitachi U-2000 or U-2000A spectrophotometer.

Mutant GFP protein (GFPuv) was purified from cells containing a commercial plasmid pGFPuv (Clontech), and used for the GFP refolding experiments in this study. *E. coli* BL21(DE3) was transformed with pGFPuv and cultivated. Purification of GFP was performed using a Resource-Q anion exchange column (GE Healthcare), Butyl-Toyopearl column (TOSOH) and Superdex 200 HR 10/30 column (GE Healthcare) in succession. Purified GFP was unfolded by acid as follows: 10 μM GFP was incubated in 0.0125N HCl containing 5 mM DTT at room temperature for 30 min. Refolding was started by 200-fold dilution of the unfolded GFP into the buffer (50 mM Hepes-KOH, pH 7.0, containing 10 mM KCl and 5 mM $MgCl_2$ or $MnCl_2$) containing 0.025–0.2 μM Ta-cpn α at 50°C. After a 5 min incubation, 1 mM (final concentration) nucleotide was added. Refolded GFP fluorescence was monitored continuously using an FP-6300 spectrofluorometer (Jasco) at 509 nm upon excitation at 473 nm. Protein concentrations of GFP during refolding were 0.05 μM, and the final fluorescence intensity of spontaneously refolded GFP was set as 100%.

ANS Fluorescence Measurements—Measurements of ANS binding fluorescence were performed on an FP-6300 fluorescence spectrophotometer (Jasco) equipped with a constant-temperature cell holder at 50°C. Ta-cpn α (0.2 μM) was mixed with ANS (final concentration; 2 μM) in 50 mM Hepes-KOH, pH 7.0, containing 10 mM KCl, in the presence or absence of either 5 mM $MgCl_2$ or $MnCl_2$. The excitation wavelength was 371 nm and the emission spectra were recorded at 400–550 nm.

Protection of Rhodanese and Luciferase from Thermal Aggregation—The ability of Ta-cpn α to protect proteins from thermal aggregation was examined using bovine liver rhodanese (*M*w 33,000, monomer) and firefly luciferase (*M*w 61,000, monomer) at 50°C. Luciferase was purchased from Promega. Thermal aggregation was started by 100-fold dilution (final protein concentration; 0.2 μM) of native rhodanese stock (20 μM in 50 mM Hepes-KOH, pH 7.0, containing 10 mM KCl, 10 mM DTT) or luciferase stock (20 μM in 50 mM Hepes-KOH, pH 7.0, containing 10 mM KCl) into reaction buffer (50 mM Hepes-KOH, pH7.0, containing 10 mM KCl and 5 mM $MgCl_2$ or $MnCl_2$) containing varying concentrations of Ta-cpn α (0–0.2 μM oligomer for rhodanese and 0–0.4 μM oligomer for luciferase). The kinetics of aggregation were monitored by light scattering using the FP-6300 spectrofluorometer (Jasco) with the emission and excitation wavelengths set to 400 nm.

RESULTS

Structural Characterization of the Recombinant Chaperonin Ta-cpn α—The structural characteristics of purified recombinant Ta-cpn α were investigated first. As the native *T. acidophilum* chaperonin is a hetero-hexadecameric complex composed of α and β subunits (*32*), we first checked to see if α subunits were able to form a quaternary structure using gel-filtration column chromatography analysis. As shown in Fig. 1A, the molecular mass of purified Ta-cpn α was about 1,000 kDa, suggesting formation of a native-like oligomeric state. In order to confirm this, we further performed TEM measurements of this complex. As shown in Fig. 1B, it was found that the Ta-cpn α chaperonin did form a ring-like complex similar to the native chaperonin (*19*, *35*, *39*). From these data, we concluded that a ring-like complex similar to that of native chaperonin from *T. acidophilum* could be formed solely from recombinant α subunits.

ATP Hydrolysis Activity of Ta-cpn α—It is well known that the ATP hydrolysis activities of chaperonins are vital to express the folding-assistance activity. The ATP hydrolysis activity of chaperonin also requires the presence of divalent metal cations, generally Mg^{2+}. However, it has been reported that Mn^{2+} ion was also effective in realizing GroEL function (*43*) as well as in stabilizing the chaperonin structure at high temperatures (*44*). Numerous researchers including ourselves have reported recently that Mn^{2+} or Co^{2+} was also critical for the ATP hydrolysis activity and the chaperonin function of various group II archaeal chaperonins (*45*, *46*). Starting from these facts, we next studied the

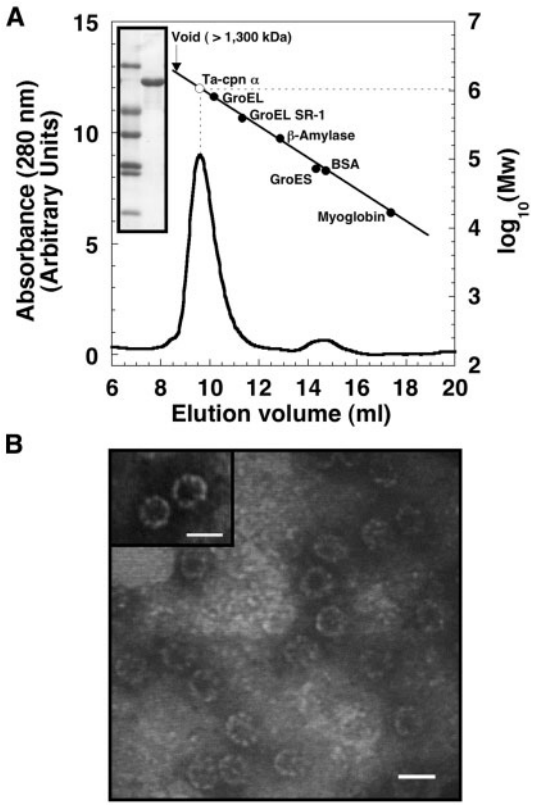

Fig. 1. **Structural characteristics of Ta-cpn α.** (A) Elution profile of purified Ta-cpn α from a Superdex 200 10/300 GL column. Closed circles, standard marker proteins plotted on a logarithmic scale (right ordinate). The arrow indicates the void volume point corresponding to molecular mass ≥1,300 kDa. Open circle indicates the elution volume of purified Ta-cpn α (~1,000 kDa). Inset: SDS–PAGE (15%-polyacrylamide gel) of purified Ta-cpn α samples (60 kDa, monomer) (right lane). Left lane; molecular markers, with molecular masses of 66.0, 45.0, 36.0, 29.0, 24.0 and 20.1 kDa, respectively, from top to bottom. (B) TEM observation of the purified Ta-cpn α. Ring structures, characteristic of chaperonins, were observed. Inset indicates a differently contrasted picture. The scale bar (both panels) indicates 10 nm.

ATP hydrolysis activity of Ta-cpn α in the presence of three different divalent cations, Mg^{2+}, Mn^{2+} or Co^{2+}, at 60°C. As shown in Fig. 2A, although Ta-cpn α exhibited a measurable ATP hydrolysis activity in the presence of each of these three divalent cations, the highest ATP hydrolysis activity was observed in the presence of Mg^{2+}. When we further investigated the hydrolysis of other nucleotides by Ta-cpn α in the presence of Mg^{2+}, we detected hydrolysis of not only ATP, but also of UTP, CTP and GTP as well (Fig. 2B). Similar specificities in nucleotide hydrolysis activity were seen for GroEL (*47*, *48*). Ta-cpn α showed no ADP hydrolysis activity.

We also found that the ATP hydrolysis activity of Ta-cpn α was enhanced greatly in the presence of NH_4^+ ion (Fig. 2C), a characteristic which was also reported for other chaperonins (*49–51*). We then examined the optimal temperature for Ta-cpn α ATP hydrolysis activity in the presence of Mg^{2+} and NH_4^+. As shown in Fig. 2D, the highest ATP hydrolysis activity was detected at 60°C, which was close to the optimal growth temperature of *T. acidophilum*.

Refolding Activity and Substrate Binding Ability of Ta-cpn α—Thermus sp. MDH as a substrate protein

We next observed the ATP-dependent protein refolding activity of Ta-cpn α at 50°C, and varied both the type of nucleotide (ATP, CTP, GTP or UTP) and the type of divalent ion that was added to the reaction (Mg^{2+}, Mn^{2+} or Co^{2+}). Figure 3 shows the refolding assistance abilities of Ta-cpn α in the presence of ATP. When MDH unfolded in Gdn-HCl was refolded by dilution into refolding buffer, an initial spontaneous yield of ~50% was seen within 2.5 min. However, the activity then gradually decreased to about 10% during the next 30 min, because MDH was unstable under these conditions. For every divalent cation tested, when the refolding reaction was started in the presence of an equimolar concentration of Ta-cpn α oligomer and 2 mM ATP, MDH recovered up to 90–100% of its initial activity during the first 5 min and this activity was maintained during the next 25 min. The relatively high yield at the initial time point was presumably due to a fast rate of refolding of the substrate protein at 50°C. The results indicated that Ta-cpn α was able to mediate the refolding of MDH in the presence of Mg^{2+}, Mn^{2+} or Co^{2+}-ATP.

Next, in order to evaluate the initial substrate binding ability of Ta-cpn α, we performed the initial dilution of denatured MDH stock solution into refolding buffer in the absence of ATP, as shown in Fig. 4. To minimize the amount of MDH intermediates that escape after binding from the chaperonin, we used an excess molar ratio of Ta-cpn α to MDH. Figure 4A shows the results of this initial trapping experiment in the presence of Mg^{2+} ion. When denatured MDH was diluted into refolding buffer containing a 6-fold molar excess of Ta-cpn α and Mg^{2+}, the MDH activity recovered during the first 5 min was about 30%, demonstrating that most of the MDH molecules had been trapped by Ta-cpn α. When ATP was subsequently added to this reaction mixture at 5 min, MDH activity was recovered nearly quantitatively over the next 30 min, indicating that ATP-dependent release of the refolding intermediates had occurred. Addition of ADP instead of ATP was not effective, *i.e.* the refolding intermediates remained trapped. This ATP-dependent refolding of MDH was also observed in the presence of Mn^{2+} (Fig. 4B) or Co^{2+} (Fig. 4C). Refolding in the presence of these two cations was characterized by differences in the refolding rate upon ATP addition, and an improved efficiency in the initial binding of refolding MDH molecules by Ta-cpn α in the absence of nucleotide (Fig. 4A–C, *triangles*). In the case of Mg^{2+}, we furthermore found that this nucleoside triphosphate-triggered release of intermediates in the presence of Mg^{2+} occurred not only upon addition of ATP but also CTP, UTP and GTP (Fig. 4D). A non-hydrolyzable ATP analogue, AMP-PNP, was not effective in refolding assistance. Hydrolysis of the nucleotides was therefore necessary. These results indicated that Ta-cpn α exhibited an ATP-dependent refolding activity of MDH in the presence of Mg^{2+}, Mn^{2+}, or Co^{2+}. In the case of Mg^{2+}, we confirmed additionally

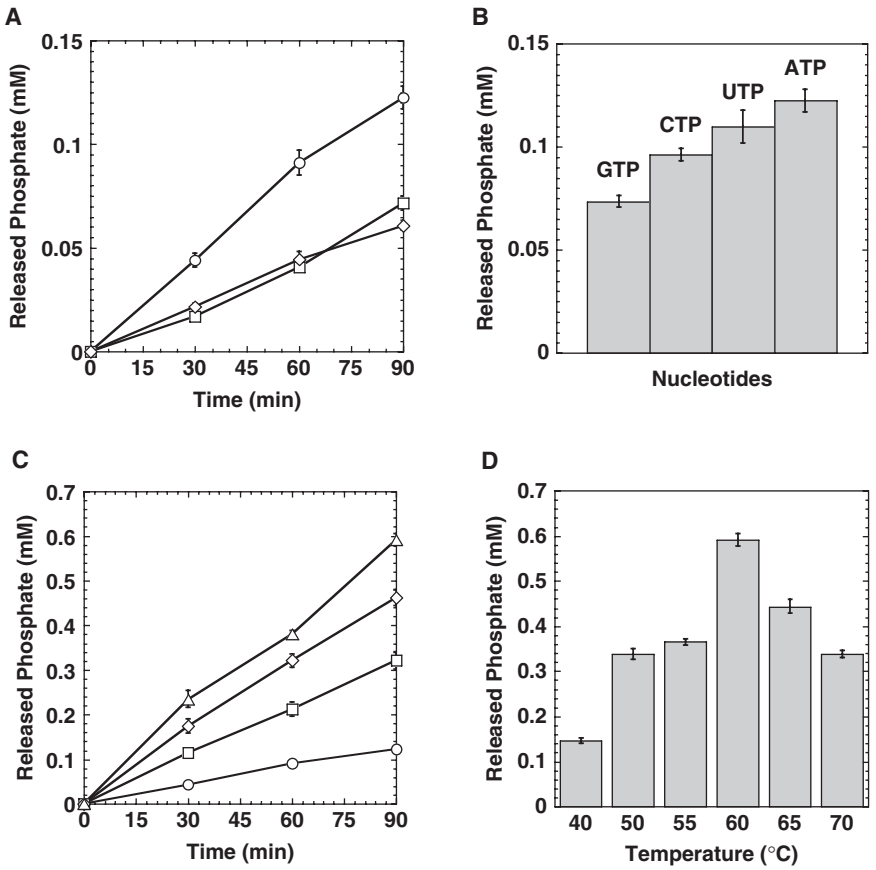

Fig. 2. **Nucleotide hydrolysis activity of Ta-cpn α.** (A) ATP hydrolysis activity in the presence of 5 mM metal ions. Circles; Mg^{2+}, squares; Co^{2+}, diamonds; Mn^{2+}. (B) Hydrolysis of ATP, UTP, CTP and GTP in the presence of 5 mM Mg^{2+}. Total phosphate released after a 90 min reaction are shown. (C) ATP hydrolysis activity in the presence of 5 mM Mg^{2+} and different concentrations of NH_4Cl. Circles; 0 mM, squares; 500 mM, diamonds; 1M and triangles; 2M. (D) ATP hydrolysis activities at various temperatures in the presence of 5 mM Mg^{2+} and 2M NH_4Cl. Total phosphate released after a 90 min reaction are shown. Error bars in the figure represent SE of the data points derived using data from at least three independent experiments.

that CTP, GTP and UTP might also initiate protein release.

GFP as a substrate protein

In order to determine if the preferences of Ta-cpn α toward nucleotides and divalent cations extended to other cases, we used GFP as a second model substrate protein. The experiments were performed in the presence of Mg^{2+} or Mn^{2+}, because under the conditions used here the addition of Co^{2+} ion caused precipitation of a DTT-cobalt adduct. GFP is a 29.5 kDa monomeric protein and the refolding reaction may be monitored directly by its fluorescence. The refolding of acid unfolded GFP was initiated by dilution into refolding buffer containing various concentrations of Ta-cpn α. As shown in Fig. 5A, when the molar ratio of Ta-cpn α to GFP was increased in the presence of 5 mM Mg^{2+}, recovery of fluorescence was suppressed. When ATP was added to the reaction mixture at $t = 5$ min, a prompt increase in the GFP fluorescence was observed, *i.e.* the trapped GFP intermediates were released by the addition of ATP. CTP, UTP and GTP were also effective in releasing GFP (data not shown). However, GFP release did not

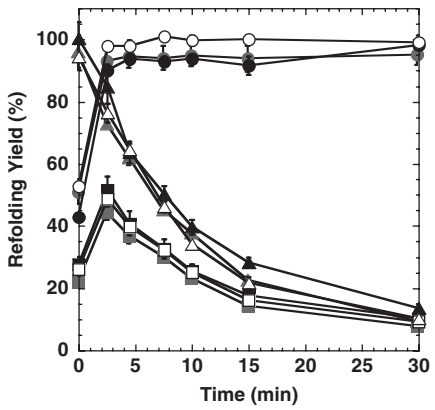

Fig. 3. **Ta-cpn α assisted refolding of *Thermus* MDH at 50°C in the presence of ATP and an equi-molar concentration of Ta-cpn α.** Refolding of MDH in the presence of an equi-molar concentration of Ta-cpn α (0.026 μM), 2 mM ATP and metal ions (circles). Spontaneous refolding (squares) and thermal stability of native MDH (triangles) under identical conditions are also presented. Black closed symbols; 5 mM Mg^{2+}, open symbols; 5 mM Mn^{2+}, gray closed symbols; 2 mM Co^{2+}. Error bars in the figure represent SE of the data points derived using data from at least three independent experiments.

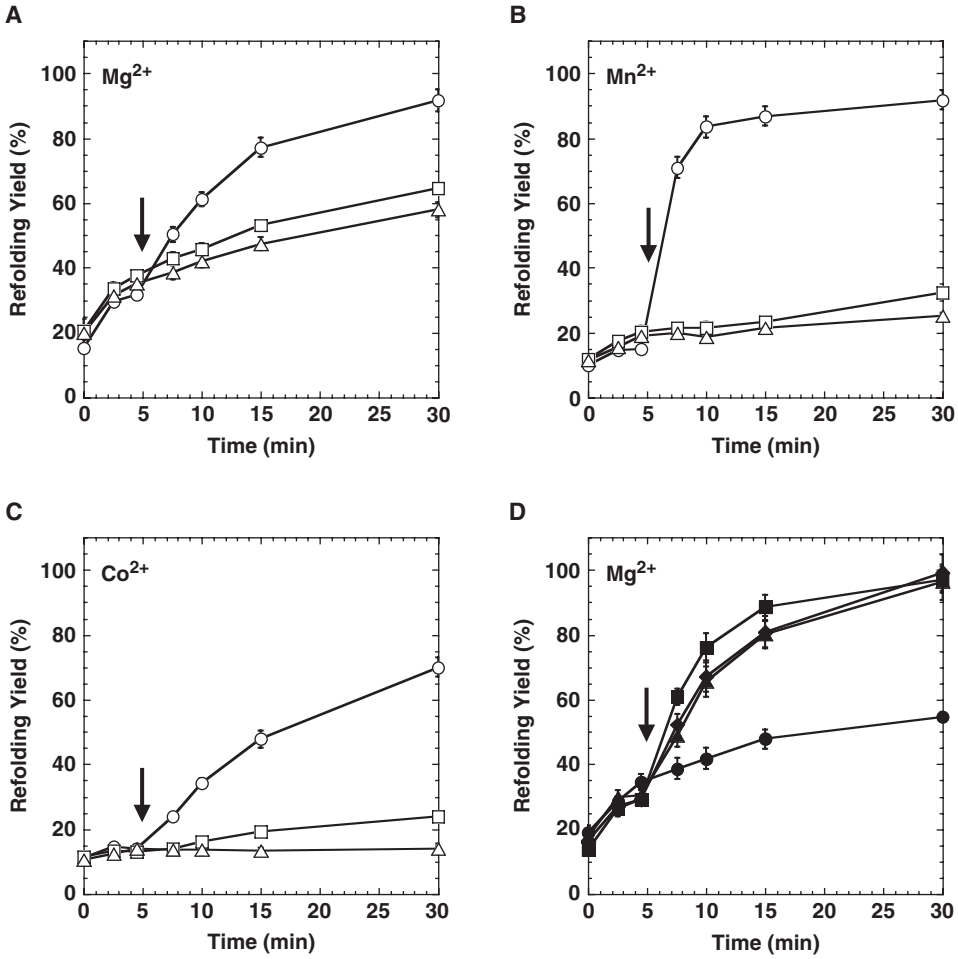

Fig. 4. **Trapping of *Thermus* MDH by Ta-cpn α and subsequent refolding at 50°C.** Refolding activity in the presence of Mg^{2+} (A), Mn^{2+} (B), and Co^{2+} (C). Final concentration of MDH was 0.026 μM. Circles; in the presence of 0.17 μM Ta-cpn α with 2 mM (final concentration) ATP added at 5 min (indicated by an arrow), squares; in the presence of 0.17 μM Ta-cpn α with 2 mM ADP added at 5 min, triangles; 0.17 μM Ta-cpn α only (no nucleotides). (D) Refolding activity in the presence of various nucleotides and Mg^{2+}. Triangles; GTP, squares; CTP, diamonds; UTP and circles; AMP-PNP. At the time indicated by an arrow, each nucleotide was added to the refolding mixture to a final concentration of 2 mM. Error bars in the figure represent SE of the data points derived using data from at least three independent experiments.

occur when either ADP or AMP-PNP was added (Fig. 5A).

We next performed analogous experiments in the presence of 5 mM Mn^{2+}. Very interestingly, as shown in Fig. 5B, we found that, similar to the behaviour observed in MDH refolding assays (Fig. 4A–B), Ta-cpn α was capable of GFP binding more efficiently in the presence of Mn^{2+} rather than Mg^{2+}; 35% of the GFP molecules present were trapped by a 2-fold excess of Ta-cpn α in the presence of Mg^{2+}, whereas 90% was trapped by the same amount of Ta-cpn α in the presence of Mn^{2+} (Fig. 5C). This finding suggested that Mn^{2+} binding transformed Ta-cpn α into a conformation that was favourable for trapping refolding substrate protein. If so, we reasoned that we should detect some differences in hydrophobicity between these two forms. To examine this, the overall hydrophobicity of Ta-cpn α in the presence of Mg^{2+} or Mn^{2+} was compared by ANS binding experiments. ANS is a probe that binds to hydrophobic patches and emits strong fluorescence (*52*). As expected, as shown in Fig. 6, ANS fluorescence intensity for Ta-cpn α in the presence of Mg^{2+} was slightly increased compared with intensities in the absence of metal ion, and fluorescence intensity in the presence of Mn^{2+} was increased even more. The result suggested strongly that binding of specific metal ions altered the conformation of Ta-cpn α into one where hydrophobic surfaces favourable for binding refolding intermediates were exposed.

Suppression of Rhodanese and Luciferase Thermal Aggregation—Chaperonins are capable of suppressing protein aggregation during thermal denaturation as well. To confirm this ability for Ta-cpn α, we investigated the suppression of thermal aggregation of bovine liver rhodanese at 50°C. In the absence of Ta-cpn α, rhodanese was denatured by heat and aggregated as detected by an increase in light scattering, as shown in Figs 7A and B. However, when a 0.25 molar ratio of Ta-cpn α oligomer was present along with Mg^{2+} in the reaction mixture,

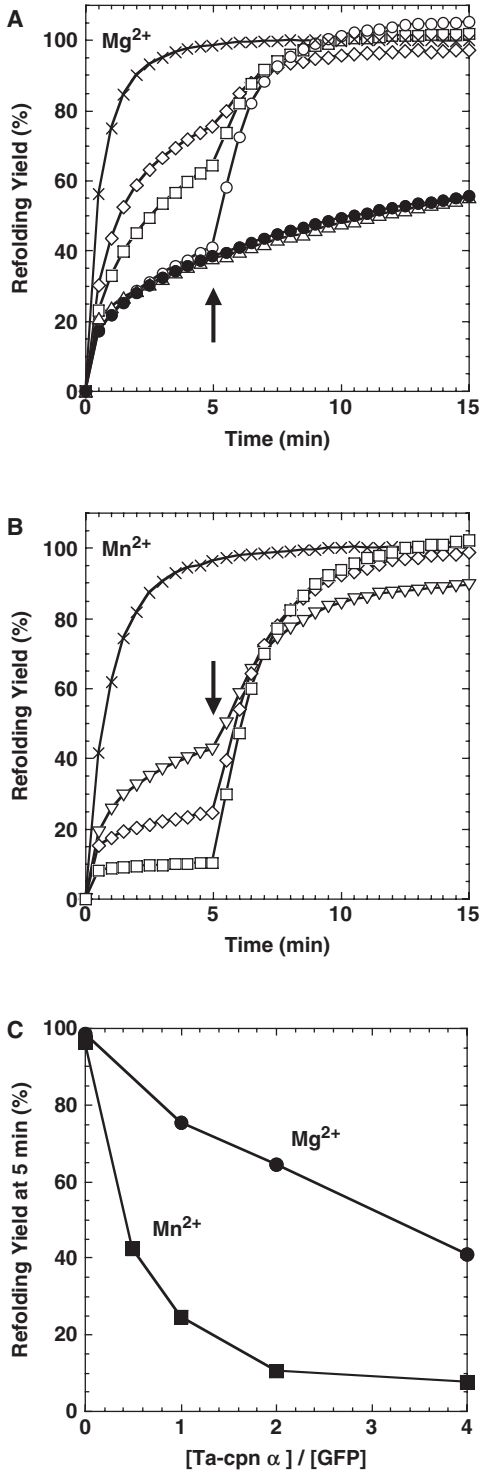

Fig. 5. **Trap and release activity of Ta-cpn α for refolding intermediates of GFP at 50°C.** GFP refolding was performed in the presence of various molar ratios of Ta-cpn α and either 5 mM Mg^{2+} (A) or Mn^{2+} (B). GFP refolding was monitored continuously by fluorescence. The final fluorescence intensity of spontaneously refolded GFP was set as 100%. Three independent experiments were averaged and shown. (A) Crosses; spontaneous refolding of 0.05 μM GFP, open diamonds; molar ratio of 1 (GFP):1 (Ta-cpn α oligomer), open squares; 1:2 and open circles; 1:4. In these reactions, at 5 min as indicated by an arrow, 1 mM ATP (final concentration) was added to the refolding mixture. For open triangles (GFP:Ta-cpn α = 1:4) and closed circles (GFP:Ta-cpn α = 1:4), 1 mM ADP and AMP-PNP were added at 5 min, respectively. (B) Inverted triangles; molar ratio of 1 (GFP):0.5 (Ta-cpn α oligomer), other symbols; same as in (A). (C) Refolding yields at 5 min in the presence of various concentrations of Ta-cpn α were plotted against the molar ratio of Ta-cpn α:GFP.

this increase in scattering intensity was retarded greatly, and when a 1.0 molar ratio was present, rhodanese aggregation was suppressed almost completely (Fig. 7A). When we performed the same experiments in the presence of Ta-cpn α oligomer and Mn^{2+}, the suppression effects were greater than for those in the presence of Mg^{2+}, as shown in Fig. 7B, which supported the notion that Mn^{2+} causes Ta-cpn α to assume a conformation that is favourable for trapping rhodanese. This suppression effect was not observed in the presence of an equi-molar concentration of bovine serum albumin (data not shown), demonstrating that this effect was specific for Ta-cpn α. In order to see if the trapped rhodanese could be subsequently refolded at a lower temperature, the Ta-cpn α: rhodanese sample initially formed at 50°C was cooled to 40°C and 2 mM ATP was added. No rhodanese activity was detected from these cooled samples, suggesting that the chaperonin could not mediate rhodanese refolding under these conditions, presumably due to a reduced ATP hydrolysis activity at lower temperatures (Fig. 2).

In order to see whether Ta-cpn α was able to bind unfolding intermediates of firefly luciferase as well as native chaperonin from *T. acidophilum* (*19*), we examined the suppression of thermal aggregation of luciferase at 50°C. As shown in Figs 7C and D, upon denaturation by heat in the absence of Ta-cpn α, luciferase was seem to aggregate as detected by an increase in light scattering. However, when an equi-molar ratio of Ta-cpn α oligomer was present along with Mg^{2+} (Fig. 7C) or Mn^{2+} (Fig. 7D) in the reaction mixture, this increase in scattering intensity was retarded greatly, and when a 2-fold molar ratio of chaperonin was present, luciferase aggregation was suppressed almost completely. This result indicated that Ta-cpn α was able to bind thermal unfolding intermediates of luciferase and suppress aggregation.

DISCUSSION

The X-ray structure of native chaperonin from *T. acidophilum* (*32*) shows that in the native chaperonin, *i.e.* the double-toroidal $(\alpha\beta)_4(\alpha\beta)_4$ form, an α subunit interacts with two β subunits at both sides of a given ring. In the present study, we demonstrated that recombinant α subunits are able to form a double-toroidal structure similar to that of the native complex (Fig. 1). However, we could not obtain a similar oligomeric protein with the purified recombinant β subunit (not shown). This suggested that the molecular recognition of α subunits towards neighbouring subunits was more tolerant than that of β subunits. The fact that we also could not obtain the native double-toroidal $(\alpha\beta)_4(\alpha\beta)_4$ structural chaperonin in recombinant form under both *in vivo* and *in vitro* conditions (*39*), suggested that some important environmental factor(s), perhaps a specific

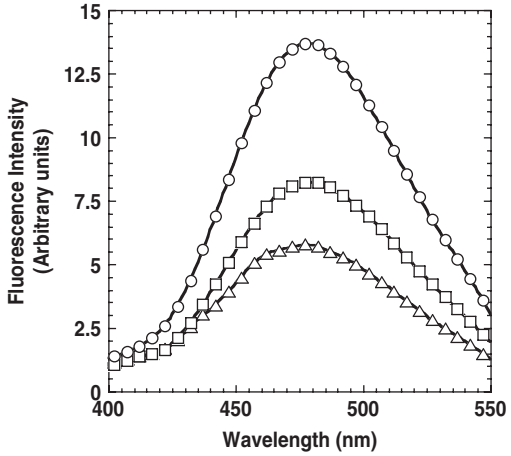

Fig. 6. **ANS fluorescence spectra of Ta-cpn α in the presence or absence of metal ion at 50°C.** Circles; 5 mM Mn^{2+}, squares; 5 mM Mg^{2+}, triangles; no metal. The concentrations of Ta-cpn α and ANS were 0.2 μM and 2 μM, respectively.

protein, might be required for native structure formation. However, we were able to obtain a homo-oligomer (Ta-cpn α) that exhibited nucleotide-dependent chaperonin function, and this allowed us to perform a more detailed characterization of the functional mechanism of archaeal group II chaperonins.

Ta-cpn α displayed ATP hydrolysis activity in the presence of not only Mg^{2+}, but also Mn^{2+} and Co^{2+} (Fig. 2). Although Mn^{2+} ion was reported to act as a substitute for Mg^{2+} in ATP-hydrolysis activities of GroEL (*43*) and *A. pernix* K1 chaperonin α (*46*), it was interesting that Ta-cpn α could hydrolyze ATP in the presence of Co^{2+} as well. This metal-dependent ATP-hydrolysis activity was demonstrated to be coupled to the MDH refolding assistance activity (Figs 3 and 4). Also, we could detect subtle differences in the relationship between nucleotide hydrolysis and refolding assistance abilities that depended on the divalent cation added. Specifically, the ATP hydrolysis activity in the presence of Mn^{2+} was lower than that in the presence of Mg^{2+} (Fig. 2A), but the rate of MDH refolding in the presence of ATP and Mn^{2+} was larger than the rate seen in the presence of ATP and Mg^{2+} (Fig. 4B). The differences may be attributed to the difference in conformational changes induced by the metal binding to the chaperonin, which was detected in further experiments (Fig. 6). In addition, we found that not only ATP, but also CTP, UTP and GTP were effective in chaperonin function, *i.e.* Ta-cpn α hydrolyzed these nucleotides and displayed nucleotide-dependent protein folding assistance abilities (Figs 2A, B, 3 and 4). It has been reported that the recombinant chaperonins from *M. maripaludis* (*51*) and *Thermococcus* strain KS-1 (*53*) exhibit nucleotide hydrolysis and protein folding activities in the presence of ATP, CTP and UTP. Taken together, these findings suggest that various metals and nucleotides may be utilized as effective factors in the function of archaeal chaperonins (*45*). This ability has also been documented to a certain extent in GroEL as well (*47*, *48*).

We detected an enhancement in Ta-cpn α ATP hydrolysis activity upon the addition of a considerably high concentration of NH_4Cl (Figs 2C and D). Since this effect was also observed upon addition of $(NH_4)_2SO_4$ (data not shown), the ammonium ion was most likely responsible for this enhancement. For several other archaeal chaperonins, it was also reported that ATP hydrolysis activity was increased by addition of ammonium ion (*49–51*). It is proposed that the presence of high concentrations of NH_4^+ induces a conformational change in the chaperonin that results in a high ATP hydrolysis activity but not in a corresponding increase in refolding-assistance ability (*34*, *54*). In agreement with this proposal, we did not observe any enhancements in the refolding-assistant functions of Ta-cpn α upon ammonium ion addition. A detailed study regarding the ATP hydrolysis activity enhancement of Ta-cpn α remains to be performed in the near future, however.

In contrast to this, we found that Ta-cpn α undergoes a conformational change in the presence of low concentrations of metal ions (Fig. 6). The conformational changes induced by binding of the metal ion to the chaperonin resulted in changes in the hydrophobicity of the surface of the chaperonin molecule with Mn^{2+} being the most effective. This conformational change to a more hydrophobic form was closely correlated to the efficiency with which Ta-cpn α could bind unfolding intermediate species of substrate proteins (Figs 4, 5 and 7). Since this effect of Mn^{2+} has also been documented for the group I chaperonin GroEL (*43*), it would seem that this effect of Mn^{2+} ion is an effect common to all chaperonin proteins.

Finally, as shown Figs 4 and 5, Ta-cpn α displayed a characteristic pattern of ATP-dependent chaperonin function; in the absence of ATP, refolding intermediates of MDH and GFP were trapped by Ta-cpn α, and upon addition of ATP, the refolding intermediates were released and refolded efficiently. Furthermore, Ta-cpn α was capable of suppressing rhodanese or luciferase aggregation caused by heat (Fig. 7). These characteristics are commonly seen in group I chaperonins such as GroEL, and a portion of group II chaperonins (*13*), but it should be emphasized that such data are still quite rare for archaeal chaperonins. In this study, we have found that Ta-cpn α chaperonin also has characteristics very similar to GroEL. This is in contrast to the results of Waldmann and co-workers (*19*), who reported that the native chaperonin from *T. acidophilum* formed a tight substrate-chaperonin complex, and did not mediate productive protein folding, even in the presence of Mg-ATP. This might be explained by the difference in substrate proteins, by the existence of β subunits, by the difference in specific ion additives such as Mn^{2+} that were revealed in the presented study, or by other unknown factors. Our experimental system using recombinant homo-oligomeric Ta-cpn α may be very important in understanding further the structural and functional characteristics of archaeal group II chaperonin.

We thank Ms Eiko Kawahara of Tottori University for assistance in TEM measurements. This work was supported in part by grants-in-aid for Scientific Research from the Ministry of Education, Culture, Sport, Science, and Technology of Japan, the Toyota Motor Corporation, and the Takeda Science Foundation.

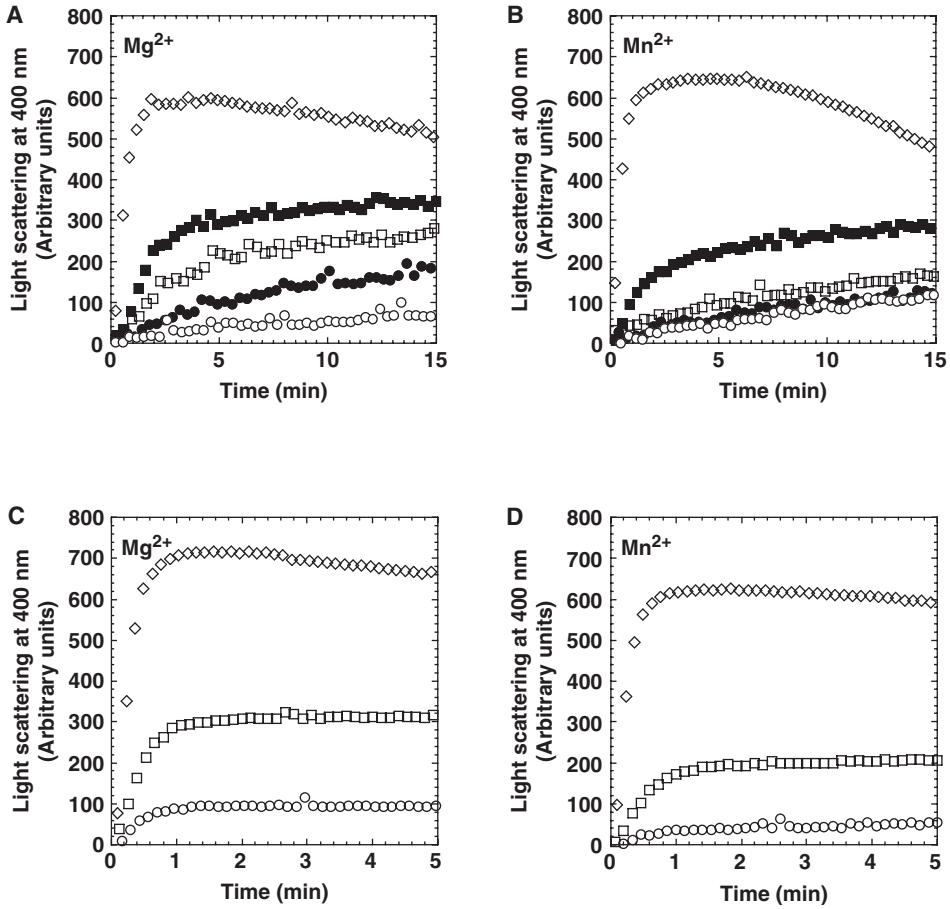

Fig. 7. **Suppression of thermal aggregation of rhodanese and luciferase by Ta-cpn α at 50°C.** (A) and (B) Suppression of thermal aggregation of rhodanese. Thermal aggregation of rhodanese was started by 100-fold dilution of 20 μM rhodanese (final concentration of rhodanese was 0.2 μM) at 50°C into the buffer containing 0–0.2 μM Ta-cpn α (oligomer) in the presence of 5 mM Mg^{2+} (A) or 5 mM Mn^{2+} (B). Diamonds; 0.2 μM rhodanese only, closed squares; in the presence of 0.05 μM Ta-cpn α, open squares; 0.075 μM Ta-cpn α, closed circles; 0.1 μM Ta-cpn α, and open circles; 0.2 μM Ta-cpn α. (C) and (D) Suppression of thermal aggregation of luciferase. Thermal aggregation of luciferase was started by 100-fold dilution of 20 μM luciferase (final concentration of luciferase was 0.2 μM) into the buffer containing 0–0.4 μM Ta-cpn α (oligomer) in the presence of 5 mM Mg^{2+} (C) or 5 mM Mn^{2+} (D) at 50°C. Diamonds; 0.2 μM luciferase only, open squares; 0.2 μM Ta-cpn α, and open circles; 0.4 μM Ta-cpn α. Aggregation reactions were monitored with a light scattering intensity at 400 nm using a fluorescence spectrofluorimeter. Three independent experiments were averaged and shown.

REFERENCES

1. Hartl, F.U. (1996) Molecular chaperones in cellular protein folding. *Nature* **381**, 571–579
2. Hartl, F.U. and Hayer-Hartl, M. (2002) Molecular chaperones in the cytosol: from nascent chain to folded protein. *Science* **295**, 1852–1858
3. Bukau, B. and Horwich, A.L. (1998) The Hsp70 and Hsp60 chaperone machines. *Cell* **92**, 351–366
4. Gutsche, I., Essen, L.O., and Baumeister, W. (1999) Group II chaperonins: new TRiC(k)s and turns of a protein folding machine. *J. Mol. Biol.* **293**, 295–312
5. Gething, M.J. and Sambrook, J. (1992) Protein folding in the cell. *Nature* **355**, 33–45
6. Mayhew, M., da Silva, A.C., Martin, J., Erdjument-Bromage, H., Tempst, P., and Hartl, F.U. (1996) Protein folding in the central cavity of the GroEL-GroES chaperonin complex. *Nature* **379**, 420–426
7. Fenton, W.A. and Horwich, A.L. (1997) GroEL-mediated protein folding. *Protein Sci.* **6**, 743–760
8. Chen, H.Y., Chu, Z.M., Ma, Y.H., Zhang, Y., and Yang, S.L. (2007) Expression and characterization of the chaperonin molecular machine from the hyperthermophilic archaeon *Pyrococcus furiosus*. *J. Basic Microbiol.* **47**, 132–137
9. Okochi, M., Matsuzaki, H., Nomura, T., Ishii, N., and Yohda, M. (2005) Molecular characterization of the group II chaperonin from the hyperthermophilic archaeum *Pyrococcus horikoshii* OT3. *Extremophiles* **9**, 127–134
10. Kowalski, J.M., Kelly, R.M., Konisky, J., Clark, D.S., and Wittrup, K.D. (1998) Purification and functional characterization of a chaperone from *Methanococcus jannaschii*. *Syst. Appl. Microbiol.* **21**, 173–178
11. Andrä, S., Frey, G., Nitsch, M., Baumeister, W., and Stetter, K.O. (1996) Purification and structural characterization of the thermosome from the hyperthermophilic archaeum *Methanopyrus kandleri*. *FEBS Lett.* **379**, 127–131
12. Furutani, M., Iida, T., Yoshida, T., and Maruyama, T. (1998) Group II chaperonin in a thermophilic methanogen, *Methanococcus thermolithotrophicus*. Chaperone activity and filament-forming ability. *J. Biol. Chem.* **273**, 28399–28407

13. Yoshida, T., Yohda, M., Iida, T., Maruyama, T., Taguchi, H., Yazaki, K., Ohta, T., Odaka, M., Endo, I., and Kagawa, Y. (1997) Structural and functional characterization of homo-oligomeric complexes of alpha and beta chaperonin subunits from the hyperthermophilic archaeum *Thermococcus* strain KS-1. *J. Mol. Biol.* **273**, 635–645
14. Atomi, H., Fukui, T., Kanai, T., Morikawa, M., and Imanaka, T. (2004) Description of *Thermococcus kodakaraensis* sp. nov., a well studied hyperthermophilic archaeon previously reported as *Pyrococcus* sp. KOD1. *Archaea* **1**, 263–267
15. Izumi, M., Fujiwara, S., Takagi, M., Kanaya, S., and Imanaka, T. (1999) Isolation and characterization of a second subunit of molecular chaperonin from *Pyrococcus kodakaraensis* KOD1: analysis of an ATPase-deficient mutant enzyme. *Appl. Environ. Microbiol.* **65**, 1801–1805
16. Minuth, T., Frey, G., Lindner, P., Rachel, R., Stetter, K.O., and Jaenicke, R. (1998) Recombinant homo- and hetero-oligomers of an ultrastable chaperonin from the archaeon *Pyrodictium occultum* show chaperone activity in vitro. *Eur. J. Biochem.* **258**, 837–845
17. Kawarabayasi, Y., Hino, Y., Horikawa, H., Yamazaki, S., Haikawa, Y., Jin-no, K., Takahashi, M., Sekine, M., Baba, S., Ankai, A., Kosugi, H., Hosoyama, A., Fukui, S., Nagai, Y., Nishijima, K., Nakazawa, H., Takamiya, M., Masuda, S., Funahashi, T., Tanaka, T., Kudoh, Y., Yamazaki, J., Kushida, N., Oguchi, A., Aoki, K., Kubota, K., Nakamura, Y., Nomura, N., Sako, Y., and Kikuchi, H. (1999) Complete genome sequence of an aerobic hyper-thermophilic crenarchaeon, *Aeropyrum pernix* K1. *DNA Res.* **6**, 83–101, 145–152.
18. Ruepp, A., Graml, W., Santos-Martinez, M.L., Koretke, K.K., Volker, C., Mewes, H.W., Frishman, D., Stocker, S., Lupas, A.N., and Baumeister, W. (2000) The genome sequence of the thermoacidophilic scavenger *Thermoplasma acidophilum*. *Nature* **407**, 508–513
19. Waldmann, T., Nimmesgern, E., Nitsch, M., Peters, J., Pfeifer, G., Müller, S., Kellermann, J., Engel, A., Hartl, F.U., and Baumeister, W. (1995) The thermosome of *Thermoplasma acidophilum* and its relationship to the eukaryotic chaperonin TRiC. *Eur. J. Biochem.* **227**, 848–856
20. Archibald, J.M., Logsdon, J.M., and Doolittle, W.F. (1999) Recurrent paralogy in the evolution of archaeal chaperonins. *Curr. Biol.* **9**, 1053–1056
21. Farr, G.W., Scharl, E.C., Schumacher, R.J., Sondek, S., and Horwich, A.L. (1997) Chaperonin-mediated folding in the eukaryotic cytosol proceeds through rounds of release of native and nonnative forms. *Cell* **89**, 927–937
22. Feldman, D.E., Thulasiraman, V., Ferreyra, R.G., and Frydman, J. (1999) Formation of the VHL-elongin BC tumor suppressor complex is mediated by the chaperonin TRiC. *Mol. Cell.* **4**, 1051–1061
23. Valpuesta, J.M., Martín-Benito, J., Gómez-Puertas, P., Carrascosa, J.L., and Willison, K.R. (2002) Structure and function of a protein folding machine: the eukaryotic cytosolic chaperonin CCT. *FEBS Lett.* **529**, 11–16
24. Camasses, A., Bogdanova, A., Shevchenko, A., and Zachariae, W. (2003) The CCT chaperonin promotes activation of the anaphase-promoting complex through the generation of functional Cdc20. *Mol. Cell.* **12**, 87–100
25. Spiess, C., Meyer, A.S., Reissmann, S., and Frydman, J. (2004) Mechanism of the eukaryotic chaperonin: protein folding in the chamber of secrets. *Trends Cell Biol.* **14**, 598–604
26. McClellan, A.J., Scott, M.D., and Frydman, J. (2005) Folding and quality control of the VHL tumor suppressor proceed through distinct chaperone pathways. *Cell* **121**, 739–748
27. Tam, S., Geller, R., Spiess, C., and Frydman, J. (2006) The chaperonin TRiC controls polyglutamine aggregation and toxicity through subunit-specific interactions. *Nat. Cell Biol.* **8**, 1155–1162
28. Kubota, S., Kubota, H., and Nagata, K. (2006) Cytosolic chaperonin protects folding intermediates of Gbeta from aggregation by recognizing hydrophobic beta-strands. *Proc. Natl. Acad. Sci. USA* **103**, 8360–8365
29. Behrends, C., Langer, C.A., Boteva, R., Böttcher, U.M., Stemp, M.J., Schaffar, G., Rao, B.V., Giese, A., Kretzschmar, H., Siegers, K., and Hartl, F.U. (2006) Chaperonin TRiC promotes the assembly of polyQ expansion proteins into nontoxic oligomers. *Mol. Cell.* **23**, 887–897
30. Kitamura, A., Kubota, H., Pack, C.G., Matsumoto, G., Hirayama, S., Takahashi, Y., Kimura, H., Kinjo, M., Morimoto, R.I., and Nagata, K. (2006) Cytosolic chaperonin prevents polyglutamine toxicity with altering the aggregation state. *Nat. Cell Biol.* **8**, 1163–1170
31. Spiess, C., Miller, E.J., McClellan, A.J., and Frydman, J. (2006) Identification of the TRiC/CCT substrate binding sites uncovers the function of subunit diversity in eukaryotic chaperonins. *Mol. Cell.* **24**, 25–37
32. Ditzel, L., Löwe, J., Stock, D., Stetter, K.O., Huber, H., Huber, R., and Steinbacher, S. (1998) Crystal structure of the thermosome, the archaeal chaperonin and homolog of CCT. *Cell* **93**, 125–138
33. Nitsch, M., Klumpp, M., Lupas, A., and Baumeister, W. (1997) The thermosome: alternating alpha and beta-subunits within the chaperonin of the archaeon *Thermoplasma acidophilum*. *J. Mol. Biol.* **267**, 142–149
34. Gutsche, I., Holzinger, J., Rössle, M., Heumann, H., Baumeister, W., and May, R.P. (2000) Conformational rearrangements of an archaeal chaperonin upon ATPase cycling. *Curr. Biol.* **10**, 405–408
35. Gutsche, I., Mihalache, O., Hegerl, R., Typke, D., and Baumeister, W. (2000) ATPase cycle controls the conformation of an archaeal chaperonin as visualized by cryo-electron microscopy. *FEBS Lett.* **477**, 278–282
36. Gutsche, I., Holzinger, J., Rauh, N., Baumeister, W., and May, R.P. (2001) ATP-induced structural change of the thermosome is temperature-dependent. *J. Struct. Biol.* **135**, 139–146
37. Bigotti, M.G. and Clarke, A.R. (2005) Cooperativity in the thermosome. *J. Mol. Biol.* **348**, 13–26
38. Bigotti, M.G., Bellamy, S.R., and Clarke, A.R. (2006) The asymmetric ATPase cycle of the thermosome: elucidation of the binding, hydrolysis and product-release steps. *J. Mol. Biol.* **362**, 835–843
39. Waldmann, T., Nitsch, M., Klumpp, M., and Baumeister, W. (1995) Expression of an archaeal chaperonin in *E. coli*: formation of homo- (alpha, beta) and hetero-oligomeric (alpha+beta) thermosome complexes. *FEBS Lett.* **376**, 67–73
40. Gutsche, I., Mihalache, O., and Baumeister, W. (2000) ATPase cycle of an archaeal chaperonin. *J. Mol. Biol.* **300**, 187–196
41. Dawson, R.M.C., Elliot, D.C., Elliot, W.H., and Jones, K.M. (1986) *Data for Biochemical Research*, 3rd edn, Clarendon Press, Oxford
42. Lanzetta, P.A., Alvarez, L.J., Reinach, P.S., and Candia, O.A. (1979) An improved assay for nanomole amounts of inorganic phosphate. *Anal. Biochem.* **100**, 95–97
43. Diamant, S., Azem, A., Weiss, C., and Goloubinoff, P. (1995) Increased efficiency of GroE-assisted protein folding by manganese ions. *J. Biol. Chem.* **270**, 28387–28391
44. Melkani, G.C., Zardeneta, G., and Mendoza, J.A. (2003) The ATPase activity of GroEL is supported at high temperatures by divalent cations that stabilize its structure. *Biometals* **16**, 479–484
45. Hongo, K., Hirai, H., Uemura, C., Ono, S., Tsunemi, J., Higurashi, T., Mizobata, T., and Kawata, Y. (2006) A novel ATP/ADP hydrolysis activity of hyperthermostable group II chaperonin in the presence of cobalt or manganese ion. *FEBS Lett.* **580**, 34–40

46. Son, H.J., Shin, E.J., Nam, S.W., Kim, D.E., and Jeon, S.J. (2007) Properties of the alpha subunit of a chaperonin from the hyperthermophilic Crenarchaeon *Aeropyrum pernix* K1. *FEMS Microbiol. Lett.* **266**, 103–109
47. Kubo, T., Mizobata, T., and Kawata, Y. (1993) Refolding of yeast enolase in the presence of the chaperonin GroE. The nucleotide specificity of GroE and the role of GroES. *J. Biol. Chem.* **268**, 19346–19351
48. Kawata, Y., Hongo, K., Mizobata, T., and Nagai, J. (1998) Chaperonin GroE-facilitated refolding of disulfide-bonded and reduced Taka-amylase A from *Aspergillus oryzae*. *Protein Eng.* **11**, 1293–1298
49. Andrä, S., Frey, G., Jaenicke, R., and Stetter, K.O. (1998) The thermosome from *Methanopyrus kandleri* possesses an NH_4^+-dependent ATPase activity. *Eur. J. Biochem.* **255**, 93–99
50. Kusmierczyk, A.R. and Martin, J. (2000) High salt-induced conversion of *Escherichia coli* GroEL into a fully functional thermophilic chaperonin. *J. Biol. Chem.* **275**, 33504–33511
51. Kusmierczyk, A.R. and Martin, J. (2003) Nested cooperativity and salt dependence of the ATPase activity of the archaeal chaperonin Mm-cpn. *FEBS Lett.* **547**, 201–204
52. Stryer, L. (1965) The interaction of a naphthalene dye with apomyoglobin and apohemoglobin. A fluorescent probe of non-polar binding sites. *J. Mol. Biol.* **13**, 482–495
53. Yoshida, T., Kawaguchi, R., and Maruyama, T. (2002) Nucleotide specificity of an archaeal group II chaperonin from *Thermococcus* strain KS-1 with reference to the ATP-dependent protein folding cycle. *FEBS Lett.* **514**, 269–274
54. Iizuka, R., Yoshida, T., Shomura, Y., Miki, K., Maruyama, T., Odaka, M., and Yohda, M. (2003) ATP binding is critical for the conformational change from an open to closed state in archaeal group II chaperonin. *J. Biol. Chem.* **278**, 44959–44965